



**Athena
SWG3
Technical Note**

Reference: SWG3.2-TN-0005
Issue : 1.1
Date : 2018-05-18
Page : 1/12

| | | | |
|-------------------|---|---------------|-----|
| Title : | Re-assessment of the performances of the optical blocking filters for X-IFU observations of massive stars | | |
| Date: | 2018-05-18 | Issue: | 1.1 |
| Reference: | SWG3.2-TN-0005 | | |

| Authors : | | Date : |
|-----------------------|--|---------------|
| G. Rauw | University of Liège, Belgium | |
| Contributors : | | |
| M. Barbera | UNIPA Dipartimento di Fisica e Chimica, Palermo, Italy | |



**Athena
SWG3
Technical Note**

Reference: SWG3.2-TN-0005
Issue : 1.1
Date : 2018-05-18
Page : 2/12

CHANGES LOG

| Issue | Date | Modifications |
|--------------|-------------|---|
| 0.0 | 2018-04-30 | Draft version of the TN |
| 1.0 | 2018-05-02 | First version to be circulated |
| 1.1 | 2018-05-18 | Updated calculations with new values of effective area and readout time |



Table of contents

| | | |
|----------|--|-----------|
| 1 | REFERENCES | 4 |
| 1.1 | REFERENCE DOCUMENTS..... | 4 |
| 1.2 | APPLICABLE DOCUMENTS..... | 4 |
| 1.3 | ACRONYMS..... | 4 |
| 2 | INTRODUCTION..... | 5 |
| 3 | WHY BOTHER ABOUT BRIGHT STARS?..... | 5 |
| 4 | SIMULATIONS | 6 |
| 5 | RESULTS..... | 8 |
| 6 | CONCLUSIONS..... | 11 |
| 7 | REFERENCES | 12 |

1 REFERENCES

1.1 REFERENCE DOCUMENTS

| Title | Reference |
|---|-----------|
| The Hot and Energetic Universe: Star formation and evolution (Sciortino, S., Rauw, G., Audard, M., et al. 2013, arXiv:1306.2333) | RD1 |
| Assessment of the performance of optical blocking filters for X-IFU observations of massive stars (Rauw, G., Barbera, M., Branduardi-Raymont, G., Oskinova, L., & Sciortino, S. 2016, SWG3.2-TN-0003) | RD2 |

1.2 APPLICABLE DOCUMENTS

| Title of the Document | Reference |
|-----------------------|-----------|
| | |

1.3 ACRONYMS

| Abbr. | Signification |
|-------|------------------------------|
| BSC | Bright Star Catalog |
| FWHM | Full Width at Half Maximum |
| PSF | Point Spread Function |
| RASS | ROSAT All Sky Survey |
| SED | Spectral Energy Distribution |
| TES | Transition Edge Sensor |
| X-IFU | X-ray Integral Field Unit |

2 INTRODUCTION

X-ray bright massive stars have been selected for in-depth studies of their X-ray spectra with the X-IFU (see RD1). Since OB stars have $\log(L_X/L_{bol}) \sim -7$ and their spectral energy distributions peak in the UV, the flux of optical and UV photons reaching the Athena telescope compared to the flux of X-ray photons can be substantial. Indeed, the X-ray brightest massive stars are also bright optical and UV targets. Optical and UV photons reaching the X-IFU focal plane lead to a degradation of the instrument's energy resolution. Therefore, in addition to the thermal filters carried by the X-IFU Aperture Cylinder, the filter wheel of the X-IFU should carry at least one optical blocking filter to attenuate the flux of non-X-ray photons. In a previous technical note (RD2), we assessed the performances of various filters for observing OB stars up to an m_V magnitude of 2 (as currently foreseen in the science plan of SWG 3.2, see RD1). Over recent months, the baseline parameters of the telescope and the X-IFU focal plane have changed. Moreover, the design of the thermal and optical blocking filters has changed as part of an exercise to optimize the effective area in the soft X-ray band. Therefore, it is time to re-consider the issue of optically bright massive stars once again.

3 WHY BOTHER ABOUT BRIGHT STARS?

To understand why we should address this issue, let us consider the distribution of bright stars with respect to their spectral types. To start, we consider Athena as an observatory, which means that any star in the sky could become at some point a potential target. We used the Bright Star Catalog to build histograms of the number of stars brighter than $m_V = 7$ as a function of spectral type. The results are shown in Fig. 1.

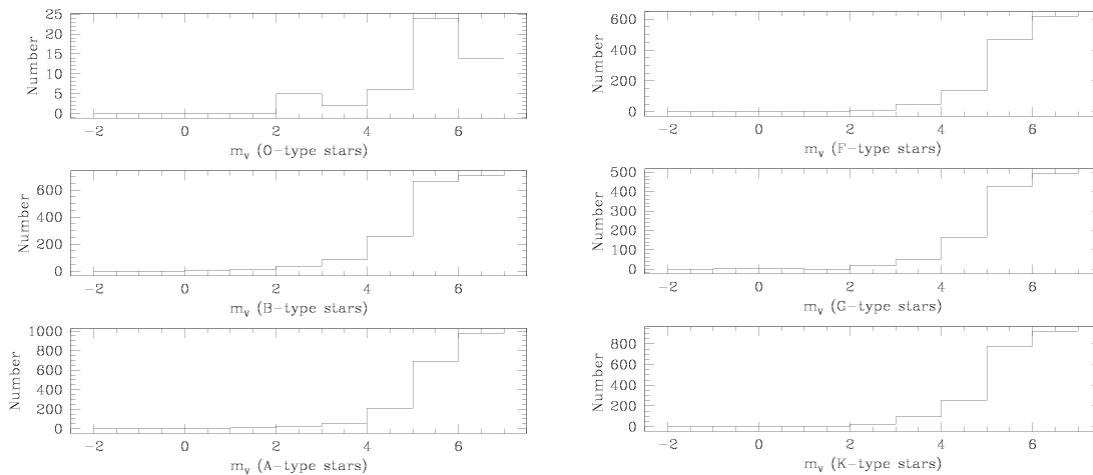


Fig. 1: Distribution of objects brighter than $m_V = 7$ in the BSC as a function of spectral type.

In a second time, we used the lists of bright/nearby stars detected in the ROSAT All Sky Survey. These objects would probably be the most interesting targets for detailed X-ray spectroscopy with X-IFU. For this purpose, we adopted the RASS sources with OB counterparts in the BSC from Berghöfer et al. (1996) and the nearby late-type stars (i.e. listed in the catalogue of Gliese & Jahreiß 1991) that are counterparts of RASS sources according to Hünsch et al. (1999). The results are shown in Fig. 2.

In RD2, we showed that a thick optical blocking filter combined with the baseline thermal filters could efficiently reject the optical load from OB stars up to a limiting magnitude of $m_V = 2$. From Fig. 2, we find that there are 21 stars (of all spectral types) brighter than $m_V = 2$ that are counterparts of X-ray

sources. In RD2, we further found that a thin optical blocking filter along with the so-called *case study 2* thermal filters would instead lead to a limiting magnitude near 6 - 7. For a limiting magnitude of $m_V \sim 6$, the number of stars that would be affected by optical load is 30 O-type stars, 165 B-stars, 27 A-stars (i.e. all but one A-star that are counterpart of a RASS source), 151 F-stars, 69 G-stars, and 26 K-stars. In the current Mock Observing Plan, there are 7 O-stars and 2 B-stars brighter than $m_V = 6$. They constitute half the sample of objects to be observed under R-SCI OBJ-325. Moreover, the X-ray timing analyses that are foreseen as part of this science objective all rely on X-ray bright sources which are also optically bright. Lacking an efficient way to suppress the optical load would essentially kill this science. There are likely other science objectives (Solar System objects and X-ray sources in Globular Clusters) where similar problems could occur.

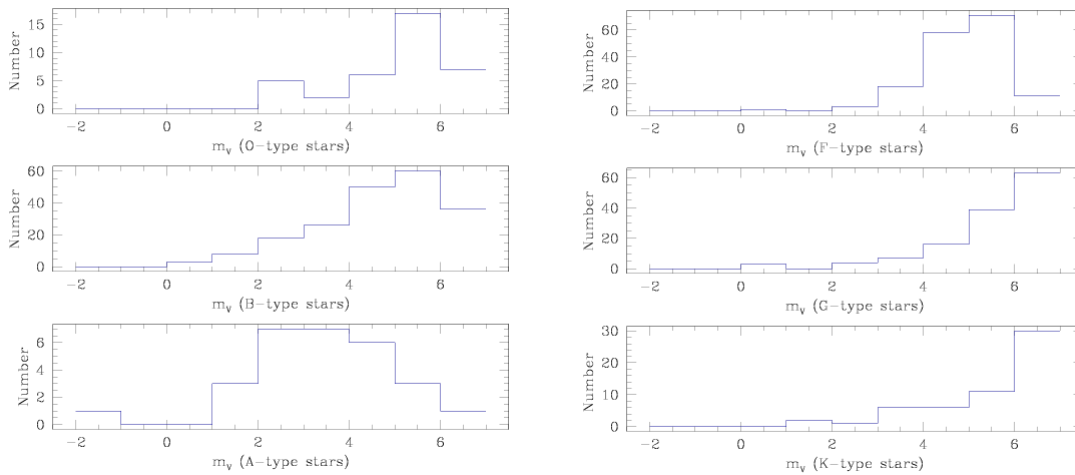


Fig. 2: Distribution of stars brighter than $m_V = 7$ that are counterparts of RASS sources as a function of spectral type.

4 SIMULATIONS

To evaluate the optical load on the X-IFU instrument when observing massive stars, we followed the same approach as in RD2. In brief, we used the TLUSTY synthetic spectra from the Ostar2002 (Lanz & Hubeny 2003) and Bstar2006 (Lanz & Hubeny 2007) grids. The Eddington fluxes of these models were converted into fluxes at Earth for a given spectral type and a given apparent magnitude. Bolometric corrections, needed for this conversion, were taken from Martins et al. (2005) for the O-type stars and Lanz & Hubeny (2007) for the B-type stars. Only main-sequence stars were considered as the relevant fluxes depend mainly on effective temperature and apparent magnitude and are not very sensitive to the surface gravity. A total of 22 temperatures between 15 000 and 45 000 K were considered and for each of them, we simulated 20 different apparent V-band magnitudes ranging from 2.0 to 11.5. We did not account for absorption by interstellar dust, but considered that absorption by the interstellar hydrogen completely blocks the stellar light below a wavelength shorter than 912 Å (in agreement with the small number of early-type stars detected in the EUVE all-sky survey, Bowyer et al. 1994).

The fluxes at Earth were integrated between 912 Å and 300 μm. For the simulations, we further assumed an effective area of the Athena telescope of 1.8 m² in the UV/optical/IR and a detector read-out time of 45 ms. In previous calculations, we had adopted the same effective area for the telescope as at 0.5 keV (1.4 m² for the “cost-compliant” mission) and a read-out time of 7.5 ms. These parameters have an important impact on the issue of optical load as we will see below.



To assess the impact of the optical load, we follow RD2 in computing the energy resolution degradation as $\Delta E_{FWHM} = 2.35 \sqrt{dt * NEP^2}$ where $NEP^2 = \int_0^\infty 2 * power(\nu) h\nu d\nu$; $dt = 0.045$ s; *power* is the power per unit frequency received by a single pixel at the focal plane of the X-IFU. We further assume that the central pixel of the PSF should receive at most 44% of the total flux of the source. At this point, let us stress that the changes in the effective area and read-out time lead to an increase of NEP^2 by a factor 7.7, hence implying an increase of the energy resolution degradation by a factor 2.8 compared to previous calculations!

Simulations were performed for different combinations of thermal filters and optical blocking filters with response curves provided by Marco Barbera for various thicknesses of polyimide and aluminium (see the table hereafter).

| | Polyimide | Aluminium |
|------------------------------|------------------|------------------|
| Single thermal filter | 45 nm | 23 nm |
| OBF option 1 | 150 nm | 23 nm |
| OBF option 2 | 150 nm | 33 nm |
| OBF option 3 | 150 nm | 43 nm |
| OBF option 4 | 150 nm | 53 nm |
| OBF option 5 | 150 nm | 63 nm |
| OBF option 6 | 150 nm | 73 nm |
| OBF option 7 | 150 nm | 83 nm |
| OBF option 8 | 200 nm | 23 nm |
| OBF option 9 | 200 nm | 33 nm |
| OBF option 10 | 200 nm | 43 nm |
| OBF option 11 | 200 nm | 53 nm |
| OBF option 12 | 200 nm | 63 nm |
| OBF option 13 | 200 nm | 73 nm |
| OBF option 14 | 200 nm | 83 nm |

To account for aluminium oxide, the transmission curve of each filter further considers that 7 nm of Al are oxidized (Al_2O_3) and are thus transparent.

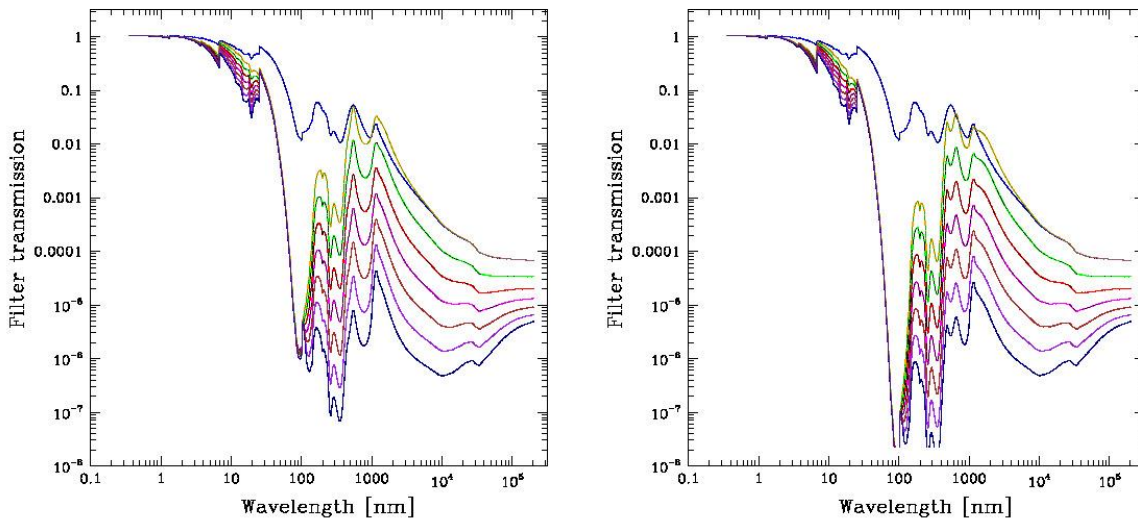
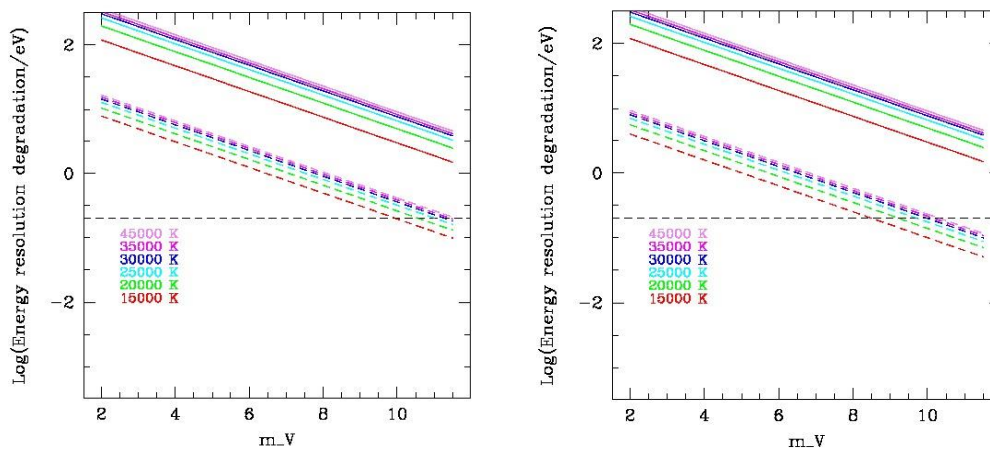


Fig. 3: Transmission curves of the various filters considered in the present study. In each figure the transmission of a single thermal filter is shown in blue. The left panel corresponds to options 1 to 7 with the various colours indicating different thicknesses of Al: orange = 23 nm, green = 33 nm, red = 43 nm, violet = 53 nm, brown = 63 nm, magenta = 73 nm, navyblue = 83 nm. Likewise, the right panel corresponds to options 8 to 14.

5 RESULTS

The results of our simulations are illustrated in Figs. 4 and 5 for a subset of the TLUSTY models (6 effective temperatures out of the 22 simulated). In each of these figures, the energy resolution degradation without auxiliary blocking filters (i.e. considering only the five thermal filters) is shown by the continuous lines, whereas the dashed lines correspond to the combination of the thermal filters with one of the options for the optical blocking filters. The acceptable level of degradation (0.2 eV see below) is shown by the dashed horizontal line.

For the filters with a layer of 150 nm of polyimide (Fig. 4), even the thickest layer of Al (option 7) is not able to completely suppress the optical load for the brightest and hottest stars.



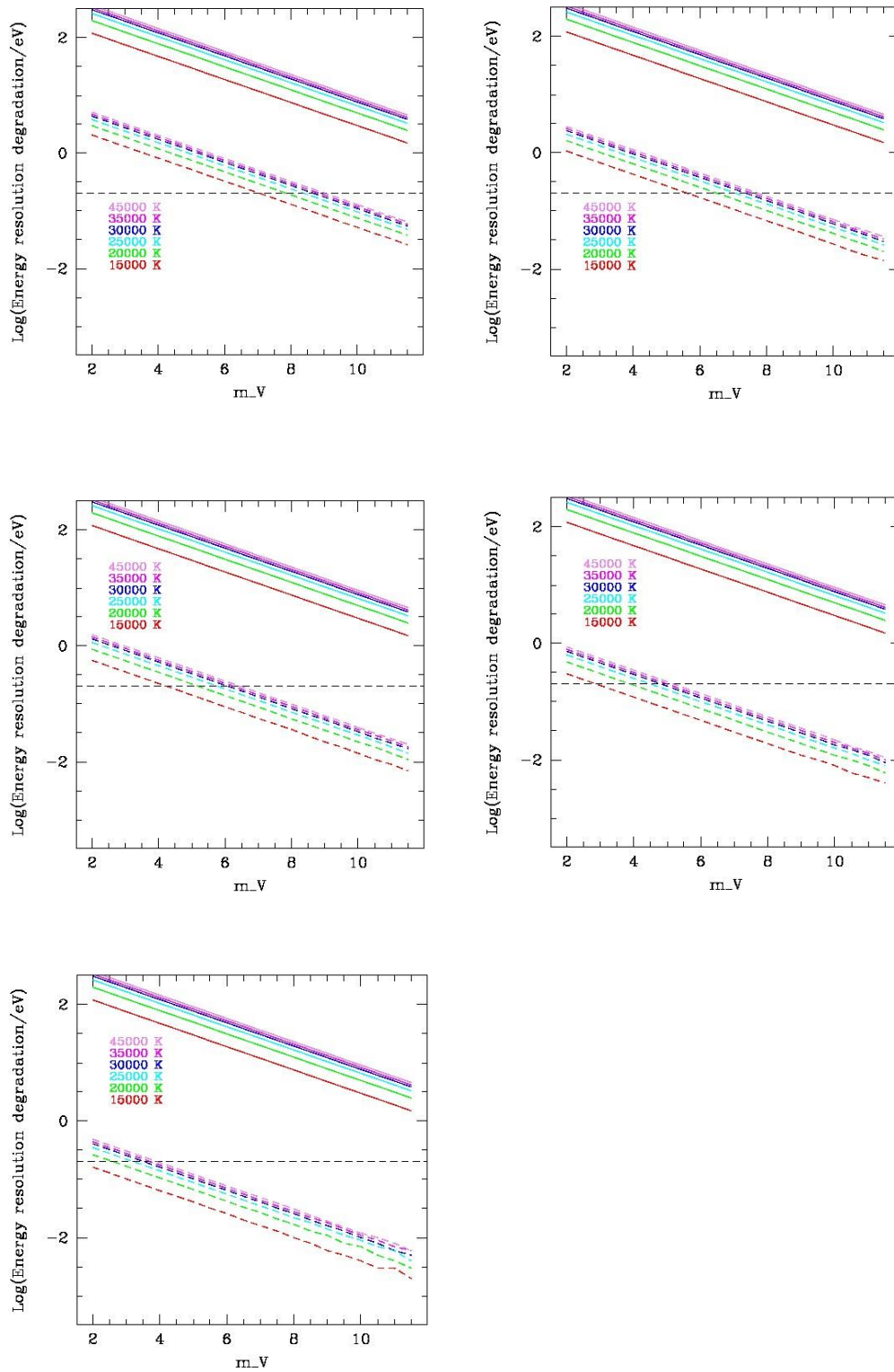
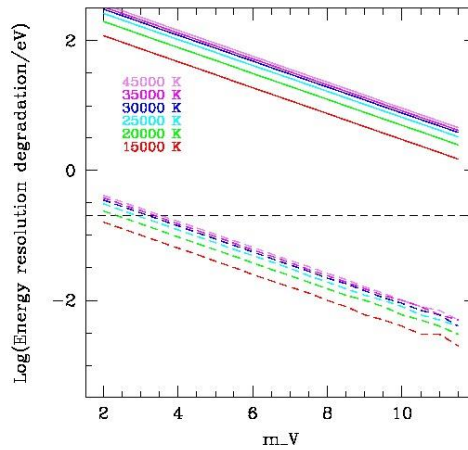
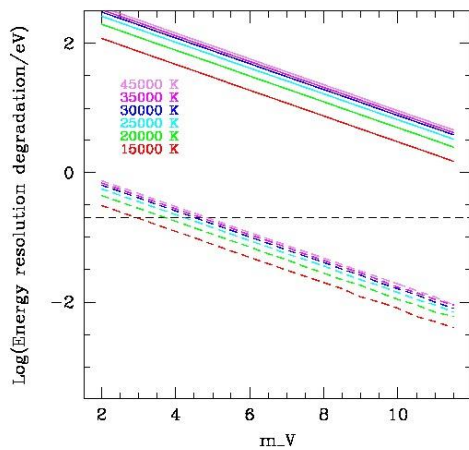
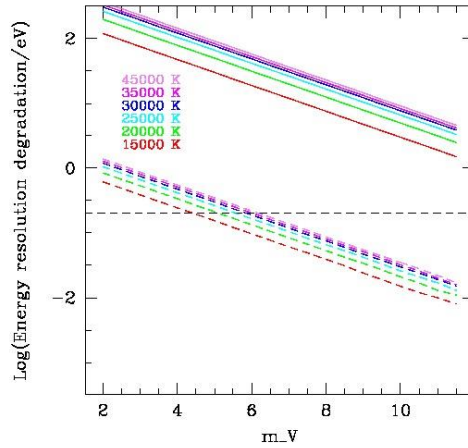
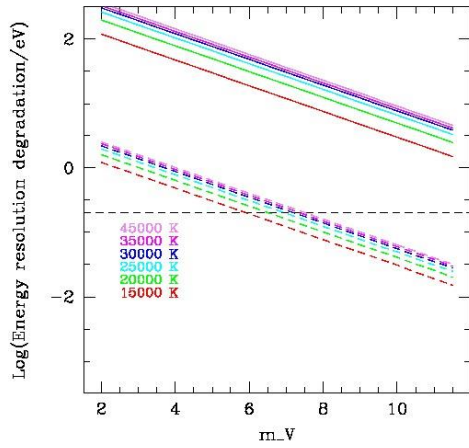
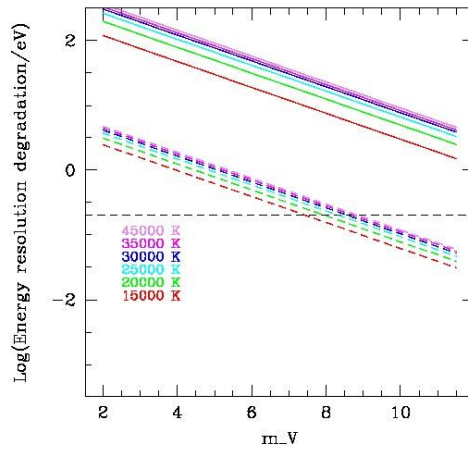
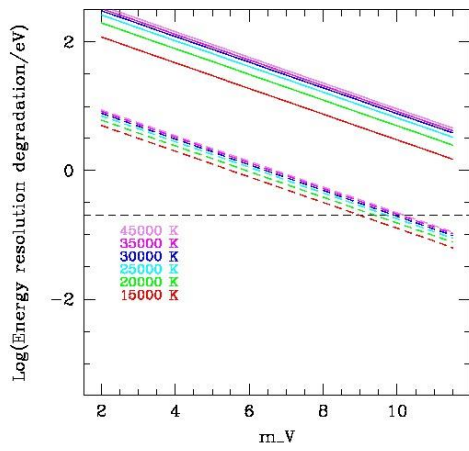


Fig. 4: Energy resolution degradation for the optical blocking filters featuring 150 nm of Polyimide. Each panel contains the results with no OBF (solid lines) whereas the dashed curves yield the results for the thermal filters combined with the OBF options 1 to 7 (from top left to bottom right).



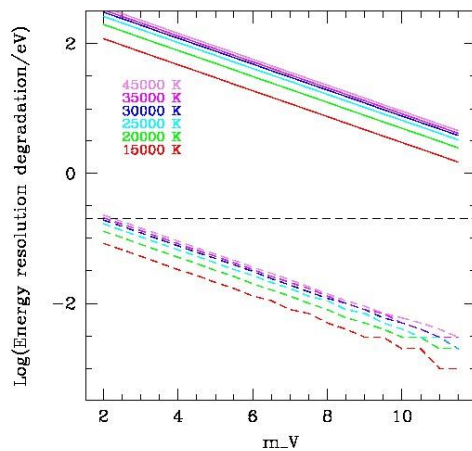


Fig. 5: Same as Fig. 4, but for the optical blocking filters featuring 200 nm of Polyimide. The dashed curves yield the results for the thermal filters combined with the OBF options 8 to 14 (from top left to bottom right).

The situation improves for options 8 to 14, although even here the thickest optical blocking filter is only just able to get rid of the optical load for the brightest and hottest stars considered here.

6 CONCLUSIONS

In conclusion, we find that with the current baseline for the collecting area and read-out time, only the very thickest auxiliary optical blocking filters allows to suppress the optical load for the brightest and hottest targets (such as ζ Puppis) foreseen in the science plans of SWG 3.2. All other options would lead to higher cut-off magnitudes.

Could we relax the 0.2 eV limit while still doing meaningful science? The degradation due to optical load is to be added in quadrature to the other effects that lead to the energy resolution. For massive stars, we need to consider two situations here. For interacting wind massive binaries, most of the science will be done with the 6.7 keV Fe lines. Considering a nominal energy resolution of 2.5 eV corresponds then to an error of 112 km s⁻¹. Simulations indicate that the Doppler maps can still be built even for an energy resolution of 4.0 keV, provided that the absolute energy calibration is known to 0.4 eV or better. Therefore, optical load up to an energy degradation of about 2 eV remains acceptable in this case. The second topic is the study of wind structures in single massive stars often associated with timing analyses. Here, the focus is on lower energy features, such as the O VIII Ly α lines at 0.65 keV. The nominal energy resolution of 2.5 eV now amounts to 1150 km s⁻¹, i.e. roughly 58% of the typical wind terminal velocity. The spectral lines will be resolved by 3 resolution elements in this case. Here a degradation of the energy resolution to 2.9 eV (corresponding to exactly 3 resolution elements over the full width of the line profile) would probably represent the worst acceptable case. Assuming no degradation of the other contributions to the energy resolution budget, we could in principle accept an energy resolution degradation due to optical load of up to 1.4 eV.

The optically brightest targets in the MOP are the targets to be observed to study stellar wind structures. If we accept a degradation of the resolution due to optical load of 1.4 eV (instead of 0.2 eV), our simulations indicate that options 5, 6, 7, 11, 12, 13 and 14 would allow to keep the degradation below this value.

| | | |
|---|---|---|
|  | Athena SWG3 Technical Note | Reference: SWG3.2-TN-0005 Issue : 1.1 Date : 2018-05-18 Page : 12/12 |
|---|---|---|

Finally, we stress that any possible measure to reduce the optical load should be taken in order to preserve a maximum scientific return.

7 REFERENCES

- Berghöfer, T.W., Schmitt, J.H.M.M., & Cassinelli, J.P. 1996, A&AS 118, 481
Bowyer S., Lieu, R., Lampton, M., et al. 1994, ApJS 93, 569
Gliese, W., & Jahreiß, H. 1991, The Astronomical Data Center CD-Rom: Selected Astronomical Catalogs Vol. I
Hünsch, M., Schmitt, J.H.M.M., Sterzik, M.F., & Voges, W. 1999, A&AS 135, 319
Lanz, T., & Hubeny, I. 2003, ApJS 146, 417
Lanz, T., & Hubeny, I. 2007, ApJS 169, 83
Martins, F., Schaerer, D., & Hillier, D.J. 2005, A&A 436, 1049
-